The effect of introducing waste heat from electrolyzers to a power plant in-between two district heating condensers.

Mohammed Abu Al-Soud[1]*, Fawzi Kayali[2], Narmin Hushmandi[3], Magnus Genrup[4]

[1]Lund University, Department of Energy Sciences, Lund, Scania, Sweden

[2] Lund University, Department of Energy Sciences, Lund, Scania, Sweden

[3]Lund University, Department of Energy Sciences, Lund, Scania, Sweden

[4]Lund University, Department of Energy Sciences, Lund, Scania, Sweden

*Corresponding Author: mohammed.abu_al-soud@energy.lth.se

ABSTRACT

The work studied the concept of introducing electrolyzer waste heat in between the district heating condensers to study the effects. This was done through IPSEpro where a model of a small-scale Swedish CHP-station was built. Two different cases were analyzed, where one CHP-station was analyzed as an existing (i.e., a fixed geometry) station and the other as a future potential station with external heat included in its design point. The components include models with the ability to be adjusted to handle off-design once set by a design point. This is meant to resemble adjusting the cycle data of an existing power plant. A pressure loss of 7 % was used for the high-pressure extraction, whilst 3 % was set for the following ones. The cycle parameters were a pressure of 140 bar, turbine inlet temperature of 540°C, and steam mass flow of 40 kg/s. This corresponds to heat input and power output of around ~97 MW and ~35 MW, respectively. The added heat between the heating stages varied between 0-10 MW, where values are 0-, 1000-, 2500-, 5000-, 7500-, and 10 000-kW. The results for a currently built CHP-station with a 10 000 kW water heating showed an increase in power output and efficiency by 70kW and 0.07 %-points, respectively, when including exhaust loss and 201kW and 0.21%-points when excluding it. The study showed an added improvement when introducing external heat in the design. This improvement, at equal heat transferred, increased power output and efficiency to 144 kW and 0.15 %-points, respectively, when including exhaust loss and 210kW and 0.22 %-points, respectively, when excluding it. When decreasing the fed external heat into the system, which was designed with external heat in mind, performance worsened once passing the 2500kW mark. The most important finding is that the heat from the electrolyzer may be introduced into a CHP station –still maintaining the required forward temperature.

1 Introduction

Sweden's first combined heat and power (CHP) station with a dedicated steam turbine was erected already in 1950 (Wickström, 2023). Since then, there has been a massive capacity buildup (Lindholm, 2024). In addition, waste heat from conventional industrial processes is also incorporated to give additional supply to the Swedish heating duty.

With the drive towards renewable energy sources, there will be an increase in demand for hydrogen. Hydrogen production requires electrolyzers and one can assume, based on current technology, that future industrial electrolyzers will have an efficiency of 60-80% (Wang, et al., 2022). Hence, 40-20 % of the used power will be available as a waste heat source. The presented work will discuss implementation strategies where the heat can be utilized in the normal district heating grid. One such is adding heat into an existing CHP station in a way that the station can always maintain a desired forward temperature.

CHP stations generally have two separate heat exchangers, in series, to minimize the exergy destruction for heating district heating water. Adding heat between these stages could lead to the benefit of a part of the steam to further expand to a lower pressure, thus increasing the power output. The reason for

https://doi.org/10.52202/077185-0201

wanting to increase the output of district heating plants is the additional power and to mitigate the volatility of increasing intermittent energy sources in the energy system while simultaneously utilizing the waste heat of an electrolyzer without a heat pump. The paper will study this concept by building a model of a small-scale Swedish CHP station in IPSEpro.

1.1 Carnot similarity

One of the main principles controlling the efficiency of a cycle is the Carnot rule. Developing and adapting the principles of the Carnot cycle to the Rankine cycles shows that increasing the average temperature of heat addition is beneficial (Kostyuk & Frolov, 1988). A higher average temperature during heat addition improves efficiency by increasing the transferred exergy (Cengel A., et al., 2020). The effect of this in the T-s diagram is an increase in the fraction of work output relative to the exhausted heat, assuming the sink temperature is constant in both cases. One of the ways to increase the average temperature of heat addition is by regenerative heating on the cold side, after the condenser, with extraction of steam from the turbine. The result is an increase in the average temperature whilst also reducing the exhaust heat. Both effects contribute to an increase in efficiency if kept within limits. Redirecting excessive amounts of steam back into the cycle will cause a reduction in steam expanding through the turbine, lowering power output and the efficiency gain.

1.2 Electrolyzer

In this paper, the waste heat source will be an electrolyzer plant. The reason is the increasing interest (in Sweden) in hydrogen as a fuel replacement for fossil fuels, especially in steel production but also potentially for heavy vehicles. The first facility is already planned to be built (Zalkalns, 2023). If the current project in Sweden finishes successfully it could pave the way for additional electrolyzer facilities.

One type of fuel cell is the conventional low temperature PEM fuel cell that operates at a temperature of around 80°C (Sharma & Pandey, 2022). This temperature is chosen to balance deterioration (worse with higher temperature) and performance (better at higher temperatures) (Zhang, et al., 2013). It is thus of high importance to stay within temperature margins by cooling the excess heat. This is achieved within a power plant by utilizing the district heating water between the condensers as a cooling source. Making use of the waste heat without the aforementioned district heating water in the power plant would require a heat pump due to the electrolyzer cooling water temperature being lower than the desired forward temperature of ~83°C (a common value in local grids).

1.3 Part-Load control

The part-load of a steam turbine can either be controlled by the throttling of pressure at the inlet varying the inlet area of the valves, thus restricting flow, or by throttling and eventually closing off an arc at the entry to the first stator (Elliott C., 1989). These two methods are known as full-arc admission and partial-arc admission, respectively. In this report, partial-arc will be chosen due to its thermodynamically superior part-load performance that stems from multiple-control valves. Having multiple control valves results in a fraction of the flow being subjected to throttling in comparison to all the flow for the full-arc admission. In addition, one could have a sliding pressure mode as an alternative but it is not included in the present work.

2 Method

2.1 Steam cycle thermodynamic model

To study the effects of including heat, a model was built in *IPSEpro*, a flexible program that uses Jacobian matrices of the model components to solve the equations. The steam cycle will be based on a small-scale older generation thermal power plant that has been producing district heating and electricity since the 90-s, see **Figure 1** below. While setting up the model, firstly, the plant will be based on general data. For the non-given data efficiency will be maximized, assuming that the real plant was done in a similar process. The maximization of efficiency will be done as a parametric study to observe the optimum values.

https://doi.org/10.52202/077185-0201

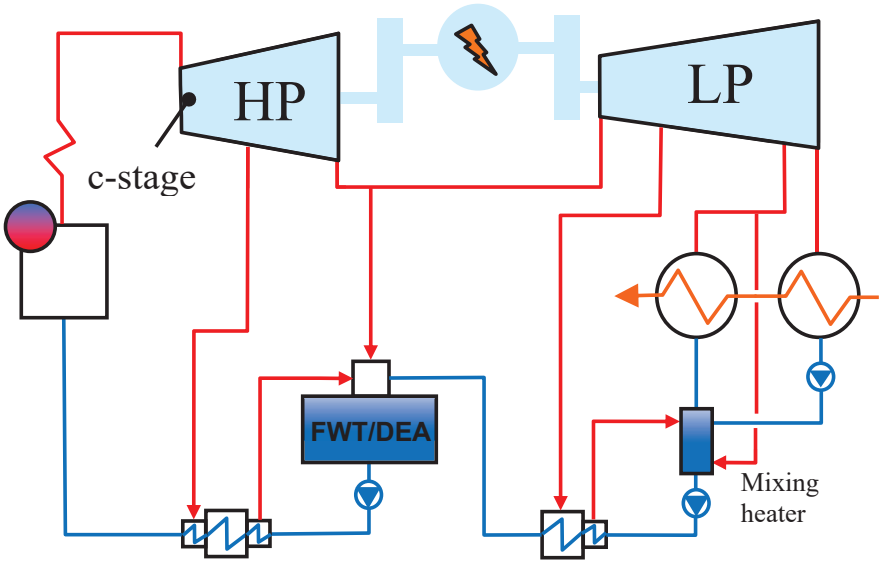

Figure 1 - A schematic of a small-scale Swedish power plant built in the 90-s.

2.2 Turbine characteristics

The turbine characteristics will also be determined from the cycle data. The characteristics is based on a variant of the Beckmann turbine equation, seen below in equation (1) (Beckmann, 1961). This equation is a modification and improvement of the swallowing capacity formula, Stodola's ellipse law. It correlates mass flow to the pressure ratio, specifc volume, and additional constants. Certain constants are chosen manually whilst cycle parameters at the design point determine the remaining ones. The only requirement to be set is the isentropic efficiency of the turbine.

$$\dot{m} = [C_t + K_\mu(\mu - \mu_{des})]\frac{(1+\mu)}{\mu}\sqrt{\frac{p_i}{v_i}}\sqrt{F} \quad (1)$$

Here, C_t is the turbine constant, K_μ being a loading constant, μ the loading of the stage(s), p_i the pressure and v_1 the inlet specific volume. F is the following,

$$F(PR,n,\lambda) = \frac{n}{n+1}\left\{1-\left[1+\frac{2\lambda}{n-1}\right](PR)^{-\frac{n+1}{n}} - \lambda\left[1-\frac{n+1}{n-1}(PR)^{-\frac{2}{n}}\right]\right\}$$

Here n represents the polytropic exponent, λ a variable that describes the loading and PR the pressure ratio of the stage(s). In this paper, K_μ will, for simplicity and without sacrificing relevance, be set to zero for all part-turbines. It could be shown that the loading is, largely, constant for all stage groups except for a control stage and the last stage.

The efficiency at the part-load/off-design for a certain number of stages is given using a correlation with the Parson number, a gauge of aerodynamic loading for blading sections. Parson number replaces the isentropic velocity ratio used for single stages (Möller F. & Genrup, 2007). Further developing the expression gives the dependence of efficiency, at an off-design point, on the ratio of isentropic enthalpy drop at the design point to the isentropic enthalpy drop at the actual running point, seen below in equation (2) (Topel, 2017). This formula is not asymptotic towards low values of isentropic enthalpy drop and, therefore, needs to be limited if low values of flow are to be analyzed, i.e., in the control stage.

https://doi.org/10.52202/077185-0201

$$\eta_s = \eta_{s,des} - 2\left(\frac{n}{n_{des}}\sqrt{\frac{\Delta h_{s,des}}{\Delta h_s}} - 1\right)^2 \quad (2)$$

Here, η_S represents the isentropic efficiency and Δh_S the isentropic enthalpy drop across the stage(s). The turbine part of the model was built by dividing the turbine into multiple separate turbines, with each turbine representing a stage or a number of stages. This was done to better model the extraction points properties, which in turn affect the cycle and its components. The chosen control of the turbine was a conventional control stage.

All turbine sections were based on the same models apart from the last stage, which included an exhaust loss model. The rationale behind this is that the kinetic energy will be utilized in the subsequent stage. The loss is different depending on whether the volume flow is increased or decreased from the design. At the design point, which is assumed to be close to the lowest loss level, the velocity at the outlet is minimized by having a well-matching flow area. When going off-design by increasing or decreasing the flow the design will not apply. This leads to the flow either going turn-up or supersonic, depending on the branch. Both introduce losses and therefore need to be modelled to accurately study changes in the cycle. Modeling the exhaust loss was done using a formula correlating the enthalpy drop to the axial velocity and a defined second axial velocity calculated using the blade speed and outlet flow angle (Möller F. & Genrup, 2007). The outlet velocity at the design point was assumed fully axial with its value set based on experience.

2.3 Deaerators and mixing heater

The model includes two deaerator components, with one being used as a mixer due to its higher number of inlets and the other being used as a deaerator. The deaerator was modeled in such a way that all inlet pressures are equal because of flashing. Thus, higher pressure condensate from extractions after heating have their pressures reduced before entering the deaerator components.

2.4 Heat exchangers

As for the feed water heaters, approximations of part-load conditions will be made. There are different approximations for high-pressure and low-pressure feed water heaters, where each is correlated to its respective design values. The high-pressure feed water heater model is a simplification of the TTD off-design behavior (Bohn & Thomas, 1985). This simplification is done due to its close-to-linear behavior which leads to a linear function of the off-design TTD dependent on the: (1.) ratio of total heat transfer at the actual running point to the design point, and (2.) the square root of mass flow ratio between the design mass flow and actual mass flow on the feedwater side. The low-pressure feed water heater model is slightly different. It is based on experience where the TTD at the actual running point relates to the ratio of mass flow at the current running point to the design point (Genrup, 2023). The ratio is multiplied by a constant and after added to another constant. The TTD for both preheaters is set at the design point, whereas it is released in part-load/off-design conditions in order to allow and observe the change in heat exchanger performance.

As for the district heating heat exchangers, an approximation was made using overall heat transfer coefficient (U) correlations and correlating this to the design value. The first heat exchanger, the coldest of the two, was modeled with a second-degree polynomial fit as a function of the cold (district heating) inlet temperature of a method proposed by the Heat Exchange Institute Standards for Steam Surface heat transfer coefficient method (El-Wakil M., 1985). The formula includes a root of velocity that needs to be given for the design point. At off-design the U is calculated by an approximated scaling with the root of mass flow ratio of the design point to the current running point. This turns into a normal ratio assuming mass-flow scales 1:1 with velocity. For the second heat exchanger, U was calculated using a polynomial fit as a function of the average district heating temperature at the inlet and outlet on the cold side (Genrup, 2023). This could not be simplified and was thus recalculated and multiplied by the root of mass flow ratios at every point. These condenser approximations are based on the fact that the cold side is dominant with the neglection of heat resistance at the tube walls. The dominance is a result of

the steam (hot) side having a complex nature in its flow with apparent turbulence combined with condensation, the combination of which disrupts heat transfer.

2.5 District heating control

Moving on to the district heating, there are multiple options of control in a power plant. The method that will be used in the studied cycle, which is also adopted at a local power station, is the control using the turbine inlet with a constant forward temperature. Responding to an increase or decrease in district heating demand is thus done by the control of the district heating mass flow.

2.6 Scenarios

2.6.1 Industrial waste heat integration: One way to increase the output for a power plant while using the excess industrial heat, as mentioned previously, could be to implement water heating between the district heating condensers in the powerplant cycle. The aim will, therefore, be an analysis oriented around the effects of implementing a specified *MW* of heat on two separate configurations. As the paper will be focused on present and future power plants, one power plant model will have its turbine characteristics set by given design point values at the extraction points and at the two district heating condensers, whilst the secondary analysis will have its characteristics set with the inclusion of waste heat in the cycle design point. Both power plant configurations will be tested off-design, where the latter is tested by decreasing the transferred heat and the former by increasing.

2.7 Final model

2.7.1 External heat source: The flow of the district heating network flows from the first condenser to the heat exchanger (HE) utilizing waste heat and finally to the second condenser. There will be a maximum temperature of the district heating water leaving the electrolyzer as a consequence of heat exchanger performance. This is set to 78°C with regards to electrolyzer cooling inlet temperature to the cycle being 82°C. To achieve this temperature level, district heating water is separated after the first condenser. One part of the fluid bypasses the external heat source whilst the other is led through it. Both streams are mixed before entering the second condenser.

2.7.2 Control stages and turbines: The control stage turbine was divided into four different parts, resembling a four-arc partial admission. These are meant to replicate the partial-arc admission inlet control. The characteristics of these turbines could not be set with the steam cycle data. This is due to the turbine downstream having its pressure set by the first feedwater heater. It is also important to have a characteristic that chokes the remaining stages once going throttling mode. If not, it can give an excessively large turbine where a decrease in pressure and flow across one valve is compensated by an increase in mass flow in the remaining turbines due to the increase in pressure ratio. To achieve an improved control by the control of pressure ratio, an additional turbine was included. The remaining turbines had their characteristics set by the cycle extraction pressures from TTD. Acquiring extraction pressures from TTD requires given temperatures after the preheaters.

2.7.3 Cycle parameters: Setting the feed water heater exit temperatures was done using parametrization and choosing the values where the cycle efficiency reached its maximum. The low-pressure feed water heater (LPFWH) exit temperatures varied from 100°C to 130°C while high-pressure feed water heater (HPFWH) exit temperatures varied from 175°C to 275°C. The maximum is found at the temperatures of LPFWH at ~120°C and ~225°C for the HPFWH. Efficiency values do not reflect the results but rather should be seen as an indication of where the maximum efficiency is attained. The temperature/pressure of the deaerator extraction was not set with parametrization and was instead chosen the same value as the replicated cycle from the 90s.
The other cycle parameter was the district heating water. It was decided to minimize the exergy loss by having an equal temperature spacing. This led to 47°C in the inlet, 65°C in-between and 83°C on the outlet. The middle temperature is released during part-load/change of cycle parameters whilst the inlet and outlet temperatures remain constant.

https://doi.org/10.52202/077185-0201

In *IPSEpro* a subcooling temperature needs to be set for heat exchangers. Sub-cooling is the temperature difference between the extraction saturated liquid temperature and the outlet condensate temperature. No large emphasis was directed towards this, because of its secondary importance, and was therefore set to 1°C. The final set parameters can be seen in **Table 1** below.

Table 1 - The final parameters that were set for the steam cycle at design point.

Parameter	Value	
Inlet pressure	140	bar
Inlet temperature	540	°C
Mass flow inlet	40	kg/s
Extraction pressure to deaerator	8	bar
Final feedwater temperature	225	°C
All component TTD	2.8	°C
Subcooling temperatures	1	°C
Low pressure feedwater feed water outlet temperature	120	°C
DH inlet/in between/outlet temperature	47/65/83	°C
Condenser 1 DH velocity	10	m/s
Pump efficiency	70	%
Part-turbine efficiency	87	%
Blade speed control-stage	400	m/s
Blade speed last stage	280	m/s
HPFWH, Deaerator and LPFWH extraction pressure loss	7/3/3	%

2.8 Validation of off-design

2.8.1 Turbine characteristics and condensers: To see whether the results are sensible off-design runs were performed. The first checks were the pressures in the cycle to study the behavior of turbine characteristics and the influence of condensers at their respective points. This was done by varying the mass flow in the cycle and noting the pressures in all the stations in between the turbines. Mass flow was lowered to a partial load of ~40 %. The plot of the results can be seen in **Figure 2** below. Here, all pressures follow a similar linear pattern apart from the last and second to last pressures, at the condenser extractions. This is what is sought since the pressures are not only controlled by the swallowing capacity formula but also by the LMTD-method. At the extractions upstream of the condenser the pressure is set by the mass flow and pressure ratio using equation (1). A decrease in mass flow is followed by a decrease in pressure due to the mass flow being inversely proportional to the pressure ratio. Moving on to the condenser pressures, the final pressure *p6* shows the correct appearance, explained in the coming parts. When going part-load, the amount of energy available in the system will decrease, leading to a decrease in district heating mass flow. This causes the slope of the district heating side in a standard T-Q diagram to increase due to its inverse proportionality of the mass flow multiplied by the isobaric heat capacity. Consequently, the temperature (and pressure) of the extraction *p6* will increase. This is illustrated **Figure 2** (right). Other work, such as (Laskowski, et al., 2020) also has this effect observable. As for the second to last pressure *p5,* an equilibrium involving the last turbine stage(s) and the second district heating condenser will be reached. The slope of the T-Q diagram will be identically affected as for the first condenser. However, a difference is the established temperature difference due to the cold side inlet and outlet temperature being set by the first condenser and the forward temperature, respectively. At part-load a smaller temperature difference will be incurred due to an increased outlet temperature from the first condenser. A smaller temperature difference combined with a reduction in district heating mass flow will cause the heat transfer and the extraction mass flow in the second condenser to decrease. The consequence of this reduction in extraction mass flow is the increase of flow entering the next turbine, resulting in an offset of turbine characteristics that increases the pressure in state 5. This effect is the reason why the slope of the pressure in state 5 is of a lower magnitude than that of the earlier extractions.

https://doi.org/10.52202/077185-0201

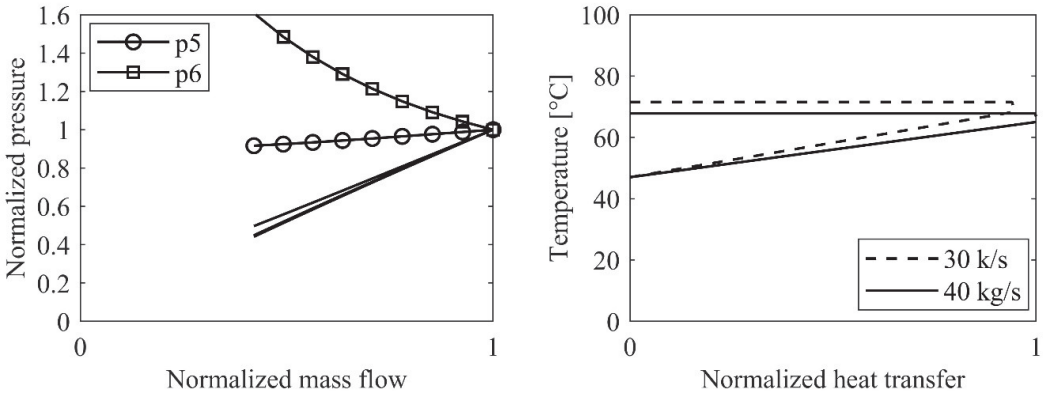

Figure 2 – Figures of the off-design results where the left shows plot of the pressures in relation to inlet mass flow (of cycle) at different points in the cycle. Numbering is done sequentially from steam inlet to outlet. The right plot shows T-Q plot of the cold condenser (first district heating condenser) for the design point 40 kg/s inlet flow (straight lines) and off-design 30 kg/s inlet flow (dashed).

For lower loads the heat transfer in the district heating condensers is thus offset towards the first district heating condenser. This is due to the extraction of the first condenser (*p6*) acquiring higher enthalpies due to higher pressures which in turn leads to a mitigation effect of the lower mass flow on the district heating side. Meanwhile, the second condenser gets a lower mass flow on the district heating side and a lower temperature difference.

2.8.2 Feed water preheater: The high-pressure preheater is modelled to follow the plots seen on the left in **Figure 3**. The approximation is linear based on the area enclosed in the red box (left). The result of this approximation is seen in the figure on the right.

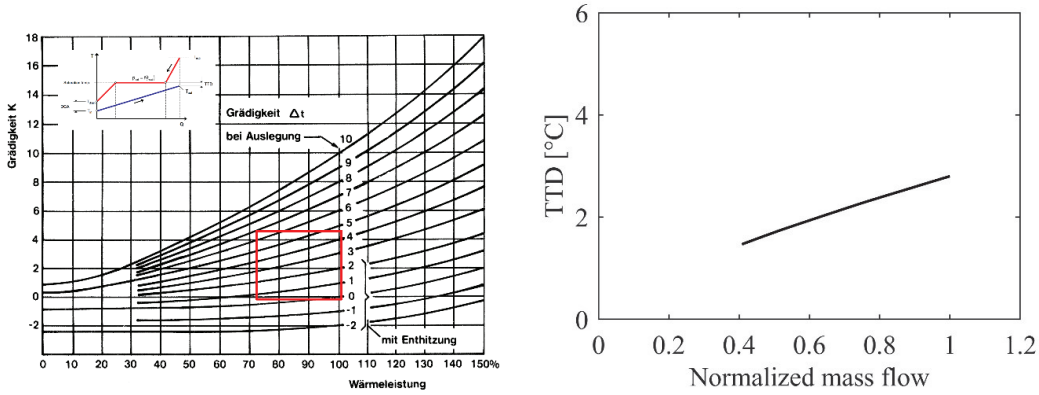

Figure 3 - The sought pattern of the high-pressure preheater that is sought (left) (Baehr, et al., 1985) and the approximation what was done (right).

3 Results

In this section the results will be presented in two different configurations where one includes the exhaust loss whilst the other does not. The application of the two configurations will be done on a present power plant and a future power plant. As mentioned previously, the present power plant is based on a fixed turbine geometry determined by the design point with no heat included. The future power plant includes this heat. For all results, the total gain in performance is compared to the base case, i.e.

https://doi.org/10.52202/077185-0201

when no external heat is added. Thus, there will be two base cases, one where the exhaust model is included and one where it is excluded.
The first condenser is based on the cold stream direction where it flows from right to left, resulting in the name DHC1 (district heating condenser 1) and DHC2.
The number of decimals varies depending on properties. To observe changes that are otherwise not clear, an additional decimal is added. In addition, some parts, such as turbine off-design resulting efficiency values, are excluded for clarity reasons.

3.1 Set cycle without included heat

3.1.1 With exhaust loss: The first study that was conducted is the inclusion of external heat flow for an existing power plant, a power plant with all its variables set at a given design point. Additionally, exhaust loss for the last stage was included. The result of this, with a focus on the condensers and their extractions, can be seen in

3.1.2

3.1.3 **Table 2** below. It followed a pattern like that during validation. The behavior is explained by the set forward temperature leading to additional heat being compensated by an increase in district heating mass flow. Increasing the mass flow results in an alteration of the T-Q charts by lowering the slope (due to inverse proportionality). A lower slope yields a decrease in temperature and pressure at the DHC1 steam extraction, resulting in a larger pressure ratio over the last stage(s). Due to the proportionality of mass flow and pressure ratio, a larger mass flow to DHC1 is attained whilst the DHC2 extraction flow is reduced. In contrast to the 'Validation' section, a small reduction in pressure was present at the DHC2 turbine extraction, even with the larger DHC1 flow. Explaining this effect is done with the principle of turbine pressures always building up from behind. A decrease in pressure at the extraction shows that the back (DHC1) pressure decreases at a faster rate in relation to the increase in pressure ratio, thus causing a mismatch that yields lower upstream pressures.
The result of including heat in this cycle was an increase in pressure ratio for the last stage (and second last stage, although minor). The total effect of these changes is observed in **Table 3** below, showing the power gained and efficiency at each external heat supply level. It can be seen that the main effects are at the last turbine stage(s) before the turbine outlet to DHC1. As for the turbine stage(s) upstream of the DHC2, power increases in a single step at 1000 kW point where it afterward starts to decrease. The reason for this is the small increase in pressure at the DHC2 extraction. This extraction is split into two where one passes the DHC2 condenser while the second provides the mixer heater with heat. The extraction pressure also sets the pressure in this mixer. A small increase in pressure results in a marginally higher temperature at the mixer outlet, requiring more heat. Due to insufficient heat from the pressure increase alone, mass flow, that expands through the turbine, is minutely increased. At greater values of transferred external heat, the reduction in pressure ratio surpasses the gains of added mass flow, resulting in a total decrease of power.

Table 2 – Results for cycle where waste heat is excluded from design, focusing on the last stages with condenser extractions. The turbines have exhaust loss enabled. Location 1 and 2 represents the first and second condenser in the direction of district heating-water stream. The subscript 'last' follows the steam path where last is the DHC1 extraction while second last is the DHC2 extraction.

$\dot{Q}_{in,external}$[kW]	$\dot{m}_{DH1}$[kg/s]	p_{DH1}[bar]	$\dot{m}_{DH2}$[kg/s]	p_{DH2}[bar]	PR_{last}[−]	$PR_{secondlast}$[−]
0	14.96	0.2837	15.5	0.5978	2.107	3.743
1000	14.98	0.2802	15.48	0.5978	2.134	3.743
2500	15.01	0.2751	15.45	0.5979	2.174	3.743
5000	15.06	0.2672	15.4	0.598	2.238	3.743
7500	15.1	0.2599	15.36	0.5981	2.301	3.742
10000	15.14	0.2532	15.32	0.5981	2.363	3.742

https://doi.org/10.52202/077185-0201

Table 3 - Summary over the cycle efficiency and net power output for the case where waste heat is not included in design while exhaust loss is. Last being before the DHC1 and second last being before DHC2.

$Q_{in,external}$ [kW]	$h_{exh,loss}$ [kJ/kg]	$P_{second,last}$ [kW]	P_{last} [kW]	η_{cycle} [%]	$\Delta\eta_{cycle}$ [%]	P_{out} [kW]	ΔP_{out} [kW]
0	28.47	5463.1	939.47	35.296	0.000	35139	0
1000	29.22	5463.3	951.70	35.303	0.007	35146	6.95
2500	30.38	5463.0	967.84	35.318	0.022	35161	22.16
5000	32.35	5462.6	989.60	35.339	0.043	35182	42.57
7500	34.37	5462.2	1005.7	35.354	0.058	35197	57.59
10000	36.42	5461.4	1017.0	35.369	0.073	35212	73.24

3.1.4 Without exhaust loss: This follows the same pattern as for the case with exhaust loss included. For this, the results are focused on the total efficiencies and gain in power in the cycle and last 2 turbine stage(s). This can be seen in **Table 4** below.

Table 4 - Summary of the cycle efficiency and net power output for the case where waste heat is not included in the design and the exhaust loss is excluded. The nomenclature is the same as earlier tables.

$Q_{in,external}$[kW]	$P_{second,last}$[kW]	P_{last}[kW]	η_{cycle}[%]	$\Delta\eta_{cycle}$[%]	P_{out}[kW]	ΔP_{out}[kW]
0	5463.1	1374.5	35.72	0.00	35557	0
1000	5463.6	1399.1	35.74	0.02	35576	19.00
2500	5463.8	1434.1	35.77	0.05	35610	53.03
5000	5464.0	1488.5	35.82	0.11	35662	105.0
7500	5464.3	1538.3	35.87	0.15	35710	153.4
10000	5464.1	1583.8	35.92	0.20	35760	202.6

3.2 Set cycle with included heat

The next cycle that was analyzed was the future power plant steam cycle, where the external heat was implemented at design. This was done in a similar manner as the previous case. Instead of increasing the external heat, it is reduced once the design point is set to study the effects of shutting it off completely. First, results of the cycle with exhaust loss will be shown and later without. The differences of the total performance (power and efficiency) will be done in relation to the corresponding case with no heat included at the design point.

3.2.1 With exhaust loss: As can be seen in **Table 5** the pattern is similar to that of the previous cases but with greater changes in pressure ratio and mass flow at the 'second, last' (DHC2) location.

Table 5 - Result focusing on the last stages with condensers with exhaust loss included for the case of external heat in design. Here location 1 and 2 is for the first and second condenser in the direction of the district heating-water stream.

$Q_{in,external}$[kW]	m_{DH1}[kg/s]	p_{DH1}[bar]	m_{DH2}[kg/s]	p_{DH2}[bar]	PR_{last}[−]	$PR_{secondlast}$[−]
0	16.97	0.3196	13.49	0.5991	1.8749	3.736
1000	17.02	0.3155	13.45	0.599	1.8986	3.7369
2500	17.09	0.3096	13.38	0.5987	1.9339	3.7382
5000	17.19	0.3004	13.28	0.5984	1.9919	3.7402
7500	17.28	0.2919	13.19	0.598	2.0489	3.7421
10000 (des)	17.36	0.284	13.1	0.5977	2.1047	3.7437

For the performance, we see a gain at the larger values of heat input but a decrease at lower ones. The turnaround happens at around 2500-kW of external heat which can be seen in **Table 6**. The gain at the

https://doi.org/10.52202/077185-0201

maximum load in comparison to the previous case is more than double that of not including heat in the design.

Table 6 - Summary over the cycle efficiency and net power output for the case with exhaust loss included. This being with external heat included in the design.

$Q_{in,external}$[kW]	$h_{exh,loss}$[kJ/kg]	η_{cycle}[%]	$\Delta\eta_{cycle}$[%]	P_{out}[kW]	ΔP_{out}[kW]
0	22.646	35.255	-0.041	35098	-41.45
1000	23.140	35.279	-0.017	35121	-17.26
2500	23.920	35.312	0.016	35155	15.98
5000	25.319	35.361	0.065	35204	64.9
7500	26.818	35.402	0.106	35245	105.8
10000 (des)	28.397	35.441	0.145	35283	144.4

3.2.2 Without exhaust loss: The results for the case of no exhaust loss can be seen in **Table 7** with the same reasoning as before only the performance will be shown. Here, the differences in comparison to the base case is minor at the maximum external heat input. Additionally, the performance is reduced when the external heat reaches values of 2 500-kW and below.

Table 7- Summary over the cycle efficiency and net power output for the case with exhaust loss excluded.

$Q_{in,external}$[kW]	η_{cycle}[%]	$\Delta\eta_{cycle}$[%]	P_{out}[kW]	ΔP_{out}[kW]
0	35.630	-0.086	35471	-85.89
1000	35.664	-0.052	35505	-52
2500	35.712	-0.004	35553	-4
5000	35.788	0.072	35629	72.05
7500	35.858	0.142	35699	141.6
10000 (des)	35.926	0.210	35767	210.1

4 Discussion

By including the heat waste in this manner, the cycle can both have the benefit of increased thermal efficiency increased output whilst also simplifying the district heating network by implementing a two-in one approach in the already existing pipe network within the power plant. The waste heat is included in the district heating network (with an increase in mass flow) whilst also giving benefits to the power plant. This avoids the added cost of a heat pump which would be needed to retain the desired forward temperature.

There is a difference between building a new power plant and including the heat supply in the design in comparison to including it in an existing facility. For the exhaust loss included, the design point is slightly improved due to the cycle parameters being optimized at this point, The result is a larger fraction of mass flow expanding through the last stages of the turbine whilst also reducing the exhaust loss leading to more than double the gain (144.4- vs 73.24-kW). Reducing the external heat supply for this design results in lower efficiency once this is below 2 500-kW. The same applies for the case where exhaust loss is excluded but with a smaller difference in power gained at the maximum heat input (209.9- vs 201.45-kW). The small differences in the gain for the case with exhaust loss excluded would result in the base cycle being chosen due to its external heat part-load performance. it is not as clear for the models with the inclusion of exhaust loss. To reach a clear conclusion, a closer economic study needs to be made regarding the uptime of the electrolyzer. If the external heat is reduced during larger fractions of power plant operation, then the benefit of building and optimizing a new facility would be nullified.

An additional analysis of different district heating temperatures could also be of interest with the chance of the effect being of a higher magnitude when larger mass flows are present in the extractions.

https://doi.org/10.52202/077185-0201

The current results are specific to the modeled power plant with a set number of assumed properties. Due to the many involved parameters, assumptions need to be made to quantify results. This can lead to uncertainty by, for example, overestimating the turbine efficiency. Stage-by-stage calculations were not made for the turbines and was instead simplified with an efficiency model. This leads to an added inaccuracy that needs to be dealt with in order to increase the feasibility of the efficiencies. Previous experience has shown that the used levels are well within expected values.

5 Conclusion

If the plan is to utilize the additional waste heat produced in an electrolyzer plant, then this would be an effective solution in both increasing the heat in the district heating network while giving benefits to an existing power plant, increasing its power output and efficiency. Exhaust loss had a major impact on the values of performance. For the case where external heat was not included in the design the performance, at 10 000-kW, was 73.24-kW additional power and 0.073 %-point increase in efficiency and 202.6-kW additional output and increase of 0.20 %-point increase in efficiency. Where the former includes exhaust loss. For the case where external heat was included in the design the calculations showed an increase of 144.4-kW, 0.145 %-points and 210-kW, 0.21 %-points in the same order with the former values including exhaust loss.

Nomenclature

C_t	Turbine constant
CHP	Combined heat and power
DH	District heating
DHC	District heating condenser
FWH	Feed water heater
h	Enthalpy [kJ/kg]
HP	High pressure
K_μ	Off-design loading constant
LMTD	Logarithmic mean temperature difference
LP	Low pressure
m	Mass flow [kg/s]
n	Polytropic exponent
p	Pressure [bar]
PEM	Proton-exchange membrane
PR	Pressure ratio
TTD	Terminal temperature difference
Greek symbols	
μ	Stage loading [-]
ν	Specific volume [m^3/kg]
λ	Stage loading factor [-]
Δ	Delta/Difference
Subscripts	
des	Design point
exh	Exhaust
s	Isentropic

References

Baehr, R. et al., 1985. Konzeption und Aufbau von Dampfkraftwerken. 5 ed. Köln: Tüv Rheinland.

Beckmann, G., 1961. *Ph.D. Dissertation; Eine allgemeine Theorie der Mengendruckgleichung,* Dresden: Von der Technischei Universität Dresden.

Bohn & Thomas, 1985. *Konzeption und Aufbau von Dampfkraftwerken.* Köln: Technischer Verlag Resch.

https://doi.org/10.52202/077185-0201

Bowman F., C. & Bowman N., S., 2020. *Thermal Engineering of Nuclear Power Stations.* Boca Raton: CRC Press.
Cengel A., Y., Boles A., M. & Kanoglu, M., 2020. *Thermodynamics, An Engineering Approach.* Singapore: McGraw-Hill.
Elliott C., T., 1989. *Standard Handbook of Powerplant Engineering.* 2nd ed. New York: McGraw-Hill.
El-Wakil M., M., 1985. *Powerplant Technology.* 2nd ed. Singapore: McGraw-Hill.
Genrup, M., 2023. *Personal Communication.* Lund: s.n.
Hushmandi B., N., 2010. *Numerical Analysis of Partial Admission,* Stockholm: KTH Royal Institute of Technology.
IEA, n.d. *Wind Energy in Sweden,* s.l.: s.n.
Jiao, K. & Li, X., 2011. Water transport in polymer electrolyte membrane fuel cells. *Progress in Energy and Combustion Science,* 37(3), pp. 221-291.
Jones-Albertus, B., 2017. *Energy.* [Online]
Available at: https://www.energy.gov/eere/articles/confronting-duck-curve-how-address-over-generation-solar-energy
[Accessed 2 November 2023].
Jonshagen, K., 2011. *Modern Thermal Power Plants, Aspects on Modelling and Evaluation. Doctoral dissertation ,* Lund: Lund University.
Kostyuk, A. & Frolov, V., 1988. *Steam and Gas Turbines.* Moscow: Mir Publishers.
Laskowski, R., Smyk, A., Rusowicz, A. & Grzebielec, A., 2020. A useful formulas to describe the performance of a steam condenser in off-design conditions. *Energy,* Volume 204.
Lindholm, K., 2024. *Energiåret - årsstatistik.* [Online]
Available at: https://www.energiforetagen.se/statistik/energiaret/
[Accessed 14 May 2024].
Möller F., B. & Genrup, M. A. M., 2007. On the off-design of a natural gas-fired combined cycle with CO2 capture. *Energy,* 32(4), pp. 353-359.
Sharma, P. & Pandey, O., 2022. *PEM Fuel Cells Fundamentals, Advanced Technologies, and Practical Application, p.2..* Amsterdam: Elsevier.
Svenska Kraftnät, 2024. *Kontrollrummet.* [Online]
Available at: https://www.svk.se/om-kraftsystemet/kontrollrummet/
[Accessed 26 January 2024].
Topel, M., 2017. *Improving Concentrating Solar Power Plant Performance through Steam Turbine Flexibility,* Stockholm: KTH Royal Institute of Technology.
Traupel, W., 2001. *Thermische Turbomaschinen.* Berlin: Springer.
Wang, Y. et al., 2022. PEM Fuel cell and electrolysis cell technologies and hydrogen infrastructure development - a review. *Energy Environ. Sci.,* 15(6), pp. 2288-2328.
Wickström, J., 2023. *Sveriges första fjärrvärmeverk firar 75 år,* s.l.: Tidningen Energi.
Zalkalns, S., 2023. *Sweden's largest electrolyzer for fossil-free hydrogen production,* s.l.: OVAKO.
Zhang, J., Zhang, H. & Wu, J., 2013. The Effects of Temperature on PEM Fuel Cell Kinetics and Performance. *Pem Fuel Cell Testing and Diagnosis,* pp. 121-141.
Zhang, J., Zhang, H., Wu, J. & Zhang, J., 2013. *PEM Fuel Cell Testing and Diagnosis.* Amsterdam, etc.: Elsevier.